Determination of the Mass Transfer Parameters and Partition Coefficients for Formic Acid/Water/Soybean Oil System

Olivieri, GV; Cogliano, T; Torres, RB; Turco, R; Salmi, T; Tesser, R; Russo, V; Di Serio, M; Giudici, R

Published in:
Industrial & Engineering Chemistry Research

DOI:
10.1021/acs.iecr.3c01562

Published: 06/09/2023

Document Version
Final published version

Document License
CC BY

I&EC research
Industrial & Engineering Chemistry Research

pubs.acs.org/IECR
Article

Determination of the Mass Transfer Parameters and Partition Coefficients for Formic Acid/Water/Soybean Oil System

Published as part of the Industrial & Engineering Chemistry Research virtual special issue "Dmitry Murzin Festschrift".

Gustavo V. Olivieri, Tommaso Cogliano, Ricardo Belchior Torres, Rosa Turco, Tapio Salmi, Riccardo Tesser, Vincenzo Russo,* Martino Di Serio,* and Reinaldo Giudici

Cite This: *Ind. Eng. Chem. Res.* 2023, 62, 13825−13836

Read Online

ACCESS | Metrics & More | Article Recommendations | Supporting Information

ABSTRACT: The formic acid partition coefficients in soybean oil/water biphasic system were determined experimentally in a Lewis cell apparatus and modeled mathematically. The effect of different operation conditions on the mass transfer parameters was investigated, i.e., temperature, water-to-soybean oil weight ratio, and formic acid-to-soybean + water weight ratio. The experimental results revealed that the temperature and water-to-soybean oil ratio bring the most relevant influence on the partition coefficient. The results were interpreted with an empirical mathematical model and two thermodynamic models, UNIQUAC (Universal Quasichemical) and NRTL (Non-Random Two Liquid). This investigation has relevance for the epoxidation of vegetable oils via the Prilezhaev concept. The approach can also be extended to other carboxylic acids, too.

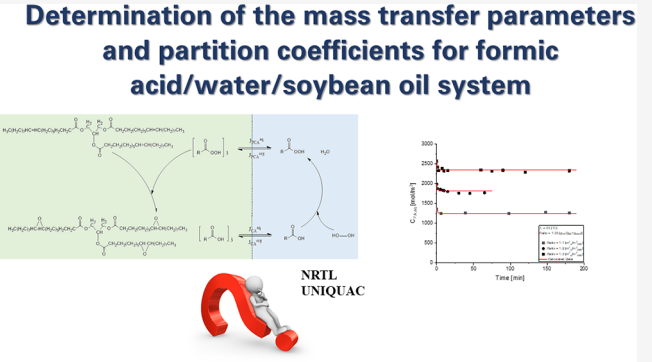

1. INTRODUCTION

Epoxidized Vegetable Oils (EVOs) have been largely employed to synthesize substances of interest as biolubricants, plasticizers, polyurethanes, and polymers.[1−9] Nevertheless, despite the high research interest in new synthesis pathways,[10−19] both the industrial production as well as the laboratory practice still rely on the Prilezhaev reaction concept. The reaction is performed in a biphasic system, where the polar phase, aqueous solution, is brought in contact with an apolar one, either a vegetable oil or its derivatives. The epoxidation synthesis takes place through a few series of steps, depicted in Figure 1.

First, a carboxylic acid reacts in the aqueous phase in the presence of either a homogeneous or heterogeneous acid catalyst with hydrogen peroxide to a percarboxylic acid. Next, the percarboxylic acid migrates from the aqueous phase to the organic phase, where it reacts with the double bonds present in the fatty acid chains of the triglyceride to epoxide. Then, carboxylic acid migrates back to the aqueous phase and reacts again with hydrogen peroxide, restarting the reaction cycle. Side reactions occur in the reaction system as well, such as decomposition of the organic peracid, and ring opening of the epoxy groups.[20−25] Thus, in the epoxidation process via the Prilezhaev reaction method, a percarboxylic acid, generally formed in situ from a carboxylic acid, is employed as an oxidizing agent thanks to its higher solubility/partition in the organic phase with respect to the hydrogen peroxide. Commonly, either acetic acid is used as a carboxylic acid. In the present paper, formic acid will be used, as the shorter the alkyl chain the faster is the percarboxylic acid formation,[26,27] thus leading to a shortening of the reaction times. In this scenario, the mass transfer from one phase to the other for both the carboxylic acid and its corresponding peracid might play a crucial role in the epoxidation process, and its impact is affected by the mass transfer coefficient and the phase equilibrium. The physical property that quantifies how a chemical component is partitioned into two either immiscible or hardly miscible phases is the partition coefficient (m), which is typically defined as the concentration ratio of the i^{th} compound in each phase. Therefore, a rigorous mathematical modeling of such a system, namely, epoxidation via the Prilezhaev concept, needs several parameters to be evaluated, among others the partition coefficient. Thus, when it is possible, the experimental determination of some of these parameters is highly preferable

Received: May 9, 2023
Revised: July 24, 2023
Accepted: August 14, 2023
Published: August 28, 2023

https://doi.org/10.1021/acs.iecr.3c01562
Ind. Eng. Chem. Res. 2023, 62, 13825−13836

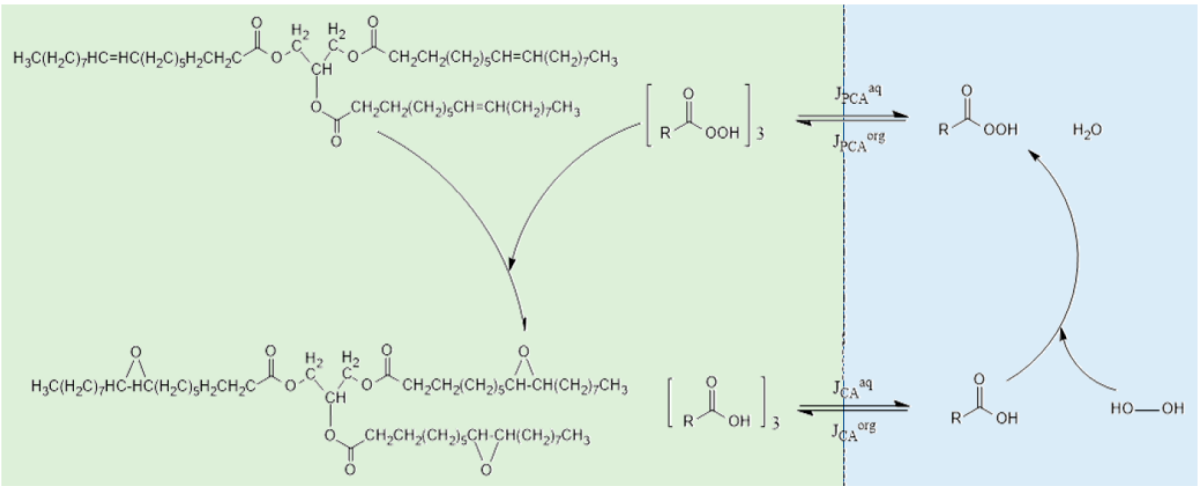

Figure 1. Reaction scheme of vegetable oil epoxidation via Prilezhaev.

and convenient, as it decreases the number of adjustable parameters to be estimated simultaneously in mathematical modeling. The correlation between the adjustable parameters is suppressed, leading to a more reliable set of parameters. Generally, in the mathematical treatment of the epoxidation system using a biphasic approach, where the partitions of the compounds in the immiscible phases is considered, the partition coefficients have been mainly estimated[28,29] or predicted through the use of an online calculator, namely, SPARC.[30−34]

Generally, the experimental determination of the partition coefficients in the epoxidation system has been carried out seldomly. Operating conditions similar to the ones used in the reaction conditions have been applied, and the effects of temperature, component ratio, and composition on the partitioning ratio have been evaluated.[35−40] Rangarajan et al.[38] determined the partition coefficient of acetic acid in a soybean oil/water system. The mixture was at first vigorously mixed for a certain time and then allowed to separate for a time as long as the mixing one. Sinadinović-Fišer and Janković[35] measured the acetic acid partition coefficient in soybean oil/water using the same experimental procedure as Rangarajan et al.[38] A wider range of temperature was investigated (i.e., from 20 to 80 °C), and the experimental data were used for predicting the partition coefficient through the use of Universal Quasichemical (UNIQUAC) as the thermodynamic model. A similar study was made from the same research group evaluating similar operating conditions but in the epoxidized soybean oil/water system.[39] From the comparison between these two investigations, it turned out that the acetic acid concentration at the equilibrium conditions increases in the oil phase in the presence of epoxidized soybean oil. A higher concentration in the oil phase in the presence of epoxidized oil was obtained also by Wu et al.[40] in the study of the formic acid partitioning ratio in a soybean-epoxidized soybean oil−water system. According to the authors, this observation is related to the presence of polar groups, namely, the epoxy group and the hydroxyl group, byproduct from the ring opening of the epoxy group which enhanced the solubility of a polar compound in the organic phase. Recently, Janković et al.[41] determined the partitions of acetic acid in a system containing linseed oil, epoxidized linseed oil, water, and hydrogen peroxide. Once again, the experimental data were used for predicting the partition coefficient with the use of a thermodynamic model.

The present study had the goal of experimentally measuring the partition coefficients of formic acid in a model system, containing soybean oil and water, at different temperatures and component proportions. The experimental apparatus was a Lewis cell, which guarantees a well-defined interfacial area between the two phases and allows one to analyze the concentration of the formic acid in the aqueous phase thoroughly along time. After the liquid−liquid equilibrium was reached, the amount of formic acid in the organic phase was analyzed. The experimental concentration profiles of formic acid in the aqueous phase were used in dynamic modeling to obtain an equation to predict the numerical value of the partition coefficient. The equation considered all of the operating parameters that affect the partition of formic acid between the two immiscible fluids. The same was done by using thermodynamic models (Non-Random Two Liquid (NRTL) and UNIQUAC). Finally, the experimental results, in terms of the absolute partition coefficient value, were compared with the values obtained by using the equation from the dynamic model developed and the value obtained from the thermodynamic models.

2. MATERIALS AND METHODS

2.1. Materials. Soybean oil (iodine value of 124 [g_{I2}/100 g_{oil}]) was purchased in a local food store; formic acid (Honeywell ≥98 [wt %]), sodium hydroxide (Carlo Erba, solid pellets), ethanol (Carlo Erba, 96% [wt %]), phenolphthalein (Merck), and distilled water were used without further purification.

2.2. Liquid−Liquid Lewis Cell. The liquid−liquid Lewis reactor consisted of a 500 mL jacketed glass reactor with an internal diameter (ID) of 6.5×10^{-2} [m], providing to a liquid−liquid interphase area (A) equal to 3.3×10^{-3} [m^2]. The reactor was equipped with a mechanical and magnetic stirrer to agitate the upper (oil) and lower (aqueous) phases, respectively. The velocity used in each experiment for both phases was kept at 50 rpm to not perturbate the liquid−liquid interphase but, meanwhile, guarantee the homogeneity in both phases. During each experiment, the reactor was at first filled up with the specific amounts of water (w_W) and formic acid (w_{FA}), and next soybean oil (w_{SBO}), according to conditions adopted for each experiment (Table 1), was added carefully to the top of the aqueous phase avoiding any mixing between the two phases. Then, the system

https://doi.org/10.1021/acs.iecr.3c01562
Ind. Eng. Chem. Res. 2023, 62, 13825−13836

Table 1. Experimental Conditions Were Adopted during the Tests

Experiment	T_r [°C]	w_W/w_{SBO}	$w_{FA}/(wW + w_{SBO})$	Experiment	T_r [°C]	w_W/w_{SBO}	$w_{FA}/(wW + w_{SBO})$
1	30	1.00	0.03	**9**	70	0.33	0.03
2	30	0.50	0.03	**10**	30	1.00	0.05
3	30	0.33	0.03	**11**	30	0.50	0.05
4	50	1.00	0.03	**12**	50	1.00	0.05
5	50	0.50	0.03	**13**	50	0.50	0.05
6	50	0.33	0.03	**14**	70	1.00	0.05
7	70	1.00	0.03	**15**	70	0.50	0.05
8	70	0.50	0.03				

was set at the operating temperature, and the two impellers were switched on. Each experiment was conducted in an isothermal mode because of the high sensitivity of the partition coefficient to temperature. The operating conditions analyzed (Table 1) were temperature (T_r), water-to-soybean oil mass ratio (w_W/w_{SBO}), and formic acid-to-soybean oil + water mass ratio ($w_{FA}/(w_{SBO}+w_W)$). The parameter values were chosen as they reproduce typical conditions for the epoxidation reaction of vegetable oil (soybean oil).

2.3. Analysis of Formic Acid. Several samples were withdrawn from the aqueous phase and analyzed via acid−base titration. The collected aqueous phase (≈0.1 [g]) was at first diluted in 10 [mL] of distilled water, and next two droplets of phenolphthalein solution were added as the indicator. The solution was titrated with a 0.1 M standardized aqueous solution of sodium hydroxide. The concentration of formic acid (C_{FA}, [mol/m^3]) was determined according to eq 1

$$C_{FA} = \frac{C_{NaOH} f_{NaOH} V_{NaOH} \rho_{sol}}{w_{sample}} \tag{1}$$

where c_{NaOH} is the sodium hydroxide solution concentration, f_{NaOH} is its correction factor, V_{NaOH} is the titrant volume needed, ρ_{sol} is the sample solution density, and w_{sample} is the sample weight. A similar analysis was carried out to measure the formic acid concentration in the organic phase ($C_{FA,org}$) just at the end of each experiment as a double-check of the real component that migrated from the aqueous phase to the organic one. A good match was obtained in every case. The procedure is practically identical with the main difference being that the titration solution was sodium hydroxide in ethanol. eq 1 was used as well to obtain the amount of formic acid in the oil phase.

2.4. Mass Balances for the Liquid−Liquid Batch System. The physical description of the system requires the solution of the mass balance equations for formic acid in both phases. As the experiments were conducted in a batch vessel, in the absence of chemical reactions, the mass balance in the aqueous and organic phases is defined, addressing exclusively the mass transfer from one phase to the other. Moreover, as the volume of each phase can be considered constant during the experimental tests, as the sample withdrawn is not affecting strongly the liquid volume, it is possible to describe the mass balance in both phases with eqs 2 & 3.

$$\frac{dC_{FA,aq}}{dt} = -J_{FA,aq} \tag{2}$$

$$\frac{dC_{FA,org}}{dt} = J_{FA,org} \tag{3}$$

The two-film theory of Whitman was considered at the liquid−liquid interphase[42] where the limitations to the diffusion from one phase to another are limited in the boundary layers in each phase. Starting from this assumption, it is possible to write the molar flux equations for formic acid in each phase.

$$J_{FA,aq} = k_{FA,aq} a_{sp} \left(C_{FA,aq} - \frac{C^*_{FA,org}}{m} \right) \tag{4}$$

$$J_{FA,org} = k_{FA,org} a_{sp} (C^*_{FA,org} - C_{FA,org}) \tag{5}$$

Here, $k_{FA,i}$ is the formic acid mass transfer coefficient in the phase "i", and a_{sp} is the specific area, equal to the ratio between the reactor cross-section area (A) and the volume in the phase "i" (V_i), as described in eq 6.

$$a_{sp} = \frac{A}{V_i} \tag{6}$$

The partition coefficient (m) is defined as the ratio between the concentration of formic acid at the interphase in the organic phase divided by the formic acid concentration at the interphase in the aqueous phase, according to eq 7.

$$m = \frac{C^*_{FA,org}}{C^*_{FA,aq}} \tag{7}$$

Considering the steady-state condition at the interphase between the formic acid molar flux to and from the organic phase, the balance reported in eq 8 can be assumed valid

$$J_{FA,aq} V_{aq} = J_{FA,org} V_{org} \tag{8}$$

from which it is possible to calculate the formic acid concentration at the interphase in the organic phase ($C^*_{FA,org}$) in agreement with eq 9.

$$C^*_{FA,org} = \frac{k_{FA,aq} a_{sp} V_{aq} C_{FA,aq} + k_{FA,org} a_{sp} V_{org} C_{FA,org}}{\frac{k_{FA,aq} a_{sp} V_{aq}}{m} + k_{FA,org} a_{sp} V_{org}} \tag{9}$$

In order to solve the system of ordinary differential equations (ODEs) (2) & (3), the value of the mass transfer coefficients ($k_{FA,i}$) and the partition coefficient (m) must be obtained by parameter estimation analysis based on the experimental data. The partition coefficient was considered dependent on both temperature and volume ratio, according to eq 10.

$$m^{-1} = a + bT + c \left(\frac{V_{aq}}{V_{org}} \right)^{-d} \tag{10}$$

According with experimental evidence obtained in the present work, as well as in the following works available on the literature,[43,44] partition coefficients have shown a strong influence on the phase volumetric ratio. Supporting this data as well as the used equation, namely, 10, it is possible to refer to Cratin[45] where, by considering the chemical potential of a compound portioned between two immiscible phases which behave ideally, it is possible to obtain the partition coefficient as a function of the ratio between the molar volumes of the two phases.

Concerning the mass transfer coefficients, we considered the mass transfer coefficients in both phases equal. Supporting this approximation, one can consider the viscosities of the two fluids. Indeed, in the temperature range investigated, the viscosities of

https://doi.org/10.1021/acs.iecr.3c01562
Ind. Eng. Chem. Res. 2023, 62, 13825−13836

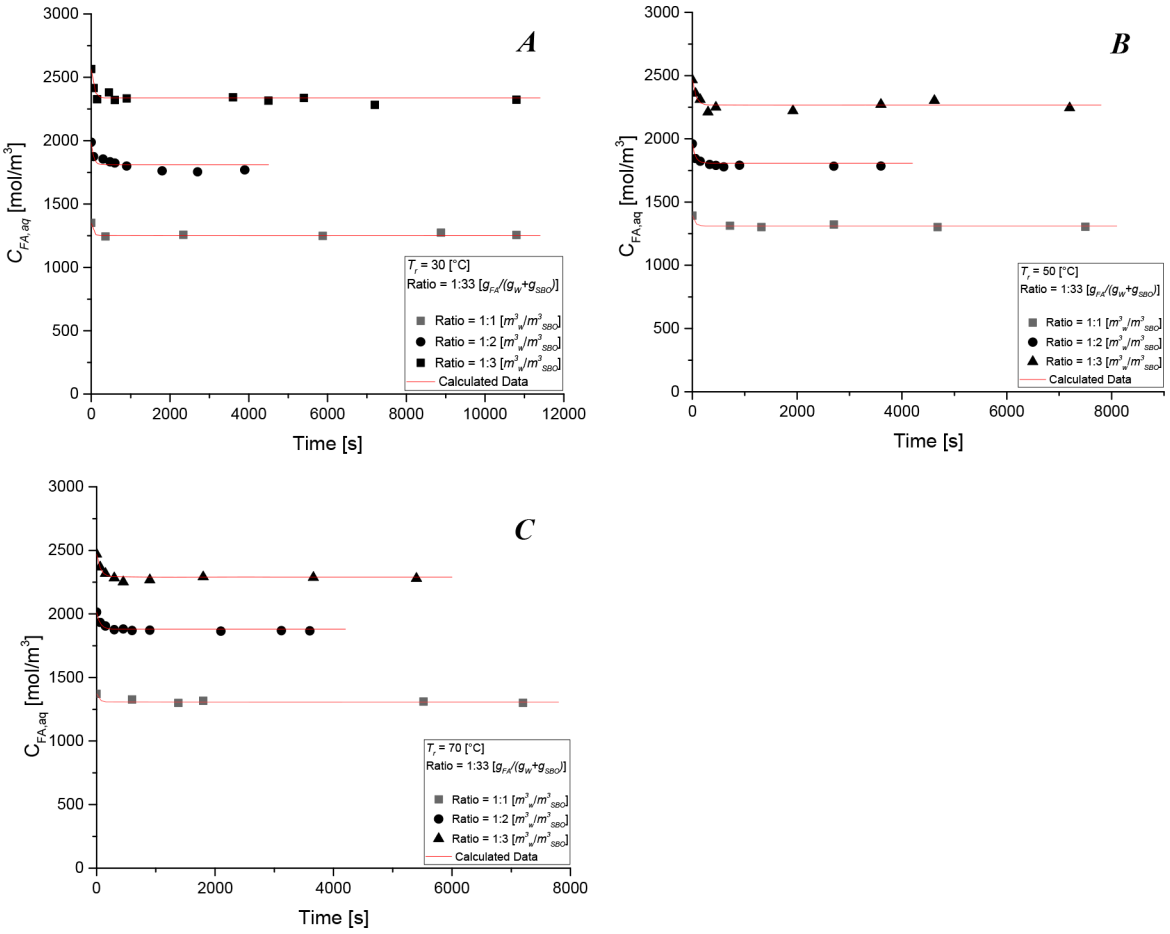

Figure 2. Fit of the mathematical model to the experimental data at different water-to-oil volume ratios (**A**) 30 [°C], (**B**) 50 [°C], (**C**) 70 [°C].

the aqueous phase and the organic phase are slightly different. Ultimately, the concentration of formic acid in the organic phase ($[FA]_{org}$) was set equal to zero as time zero condition.

2.5. Numerical Strategies. The system of ODEs (2) & (3) was solved with MatLab R2022b as software using the *ode23s* built-in function. The parameter estimation activities were conducted by using the deterministic minimization algorithm *lsqnonlin*. For each parameter, the confidence interval at 95% was calculated with the *nlparci* built-in function. Finally, the covariance matrix (V) and the correlation matrix (Cor_{ij}) were evaluated to check the correlations between the adjustable parameters, according to eqs 11 and 12.

$$V_{ij} = s^2(JJ)'^{-1} \tag{11}$$

Here, s denotes the standard deviation of residues, and J and J' are the Jacobian matrix and its transpose, respectively. The elements of the correlation matrix are evaluated according to eq 12.

$$\mathrm{Cor}_{ij} = \frac{V_{ij}}{\sqrt{V_{ii}}\sqrt{V_{jj}}} \tag{12}$$

Finally, the agreement between the experimental and predicted data is evaluated by statistical analysis based on the adjusted coefficient of determination (R_{Adj}^2)

$$R_{\mathrm{Adj}}^{\ 2} = 1 - \frac{n-1}{n-k-1}\frac{\sum_{i=1}^{N}(y_i - \hat{y}_i)^2}{\sum_{i=1}^{N}(y_i - \bar{y})^2} \tag{13}$$

where n denotes the number of experimental observations, k is the number of adjustable parameters, N is the number of experimental tests, $\bar{y}$ is the average value of the experimental observation, and y_i and $\hat{y}_i$ are the values of the experimental and calculated observation at the i^{th} experiment, respectively.

2.6. Thermodynamic Modeling. Two thermodynamic models for activity coefficients were employed to adjust the partition coefficient results: UNIQUAC (Universal Quasichemical) and NRTL (Non-Random Two Liquid).[46] In order to do that, the partition coefficients calculated by the models followed eq 14

$$m = \frac{\rho_{m,\mathrm{org}} x_{\mathrm{FA,org}}}{\rho_{m,\mathrm{aq}} x_{\mathrm{FA,aq}}} \tag{14}$$

where $x_{FA,j}$ is the molar fraction of formic acid and $\rho_{m,j}$ is the molar density of the j phase.

The molar densities of each phase were approximated to the molar densities of water (for the aqueous phase) and soybean oil (for the organic phase)

$$\rho_{m,\mathrm{aq}} = \frac{\rho_{\mathrm{W}}}{M_{\mathrm{W}}} \tag{15}$$

$$\rho_{m,\mathrm{org}} = \frac{\rho_{\mathrm{SBO}}}{M_{\mathrm{SBO}}} \tag{16}$$

in which M_W and M_{SBO} are the molar masses of water and soybean oil, respectively, and the mass densities (ρ_W and ρ_{SBO}) were expressed as a function of the temperature (T_r), based on

https://doi.org/10.1021/acs.iecr.3c01562
Ind. Eng. Chem. Res. 2023, 62, 13825−13836

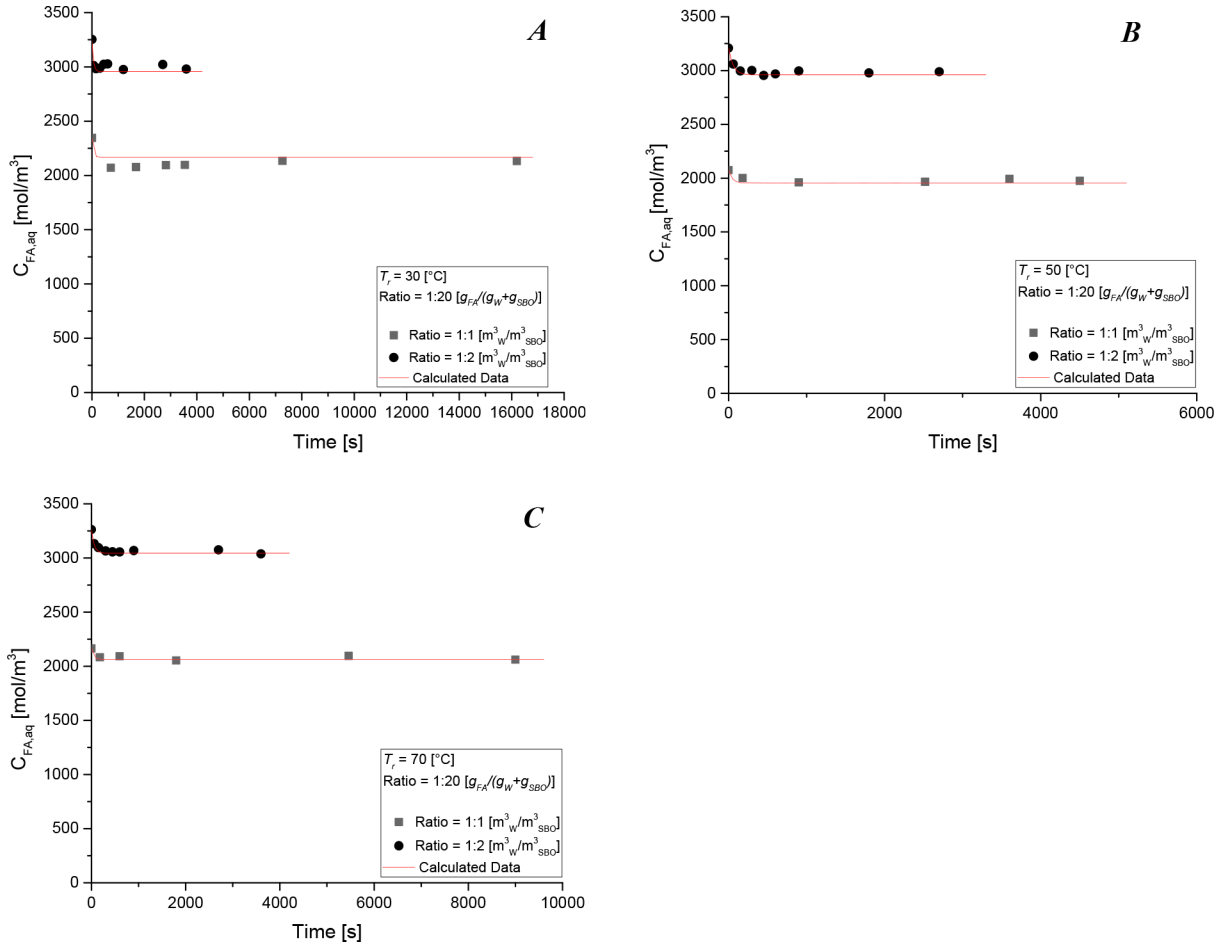

Figure 3. Fit of the mathematical model to the experimental data at different water-to-oil volume ratios (**A**) 30 [°C], (**B**) 50 [°C], (**C**) 70 [°C].

literature data.[47,48] The molar mass of soybean oil was estimated as 862 g/mol.

A phase equilibrium relation is introduced in eq 17, in order to correlate the molar fractions and the activity coefficients (γ) of formic acid in each phase.[46]

$$\gamma_{FA,aq} x_{FA,aq} = \gamma_{FA,org} x_{FA,org} \tag{17}$$

The substitution of eq 17 into (14) leads to eq 18.

$$m = \frac{\rho_{m,org}\gamma_{FA,aq}}{\rho_{m,aq}\gamma_{FA,org}} \tag{18}$$

The Supporting Information section details the equations employed by the models considered. In the present study, UNIQUAC uses four adjustable parameters (characteristic energies Δu), while NRTL works with four adjustable parameters (characteristic energies Δg) and two parameters α related to the nonrandomness of the mixtures that were considered as constant values equal to 0.3.[46] The adoption of this value for the nonrandomness parameters also occurred in similar studies in the literature.[49−51]

The estimation of the parameters considered the following objective function (OF)

$$\mathrm{OF} = \min_{\text{parameters}} \sum_{i=1}^{N} (y_i - \hat{y}_i)^2 \tag{19}$$

where N is the number of experimental tests, y_i and $\hat{y}_i$ are the values of the experimental and calculated observation of the partition coefficients at the i^{th} experiment, respectively.

The adjusted coefficient of determination was calculated for both models according to eq 13.

3. RESULTS AND DISCUSSION

3.1. Results of the Partition Experiments. The first set of experiments was devoted to the investigation of the water-to-soybean oil weight ratio effect, keeping constant both the temperature and formic acid-to-soybean+water weight ratio (Table 1, entries 1−3). This set of experiments was conducted at higher temperatures, too, at 50 and 70 [°C] to verify how the temperature influences the partition coefficient (Table 1, entries 4−9). Finally, the formic acid-to-soybean+water weight ratio was increased, and experiments were conducted at 30, 50, and 70 [°C] with an amount of water-to-oil weight ratio equal to 1 and 0.5, respectively (Table 1, entries 10−15).

As the total amount of water and soybean oil (in weight) was kept constant and equal to 0.40 [kg], by decreasing the water-to-oil weight ratio with a fixed amount of formic acid-to-soybean +water, the concentration of formic acid in the aqueous phase increased. Consequently, the initial concentration of formic acid in the aqueous phase ($C_{FA,aq}$) at zero time increases with a lower water-to-oil weight ratio. Indirectly, when the water-to-oil weight ratio is changed, the volume ratio between the two phases changes as well.

https://doi.org/10.1021/acs.iecr.3c01562
Ind. Eng. Chem. Res. 2023, 62, 13825−13836

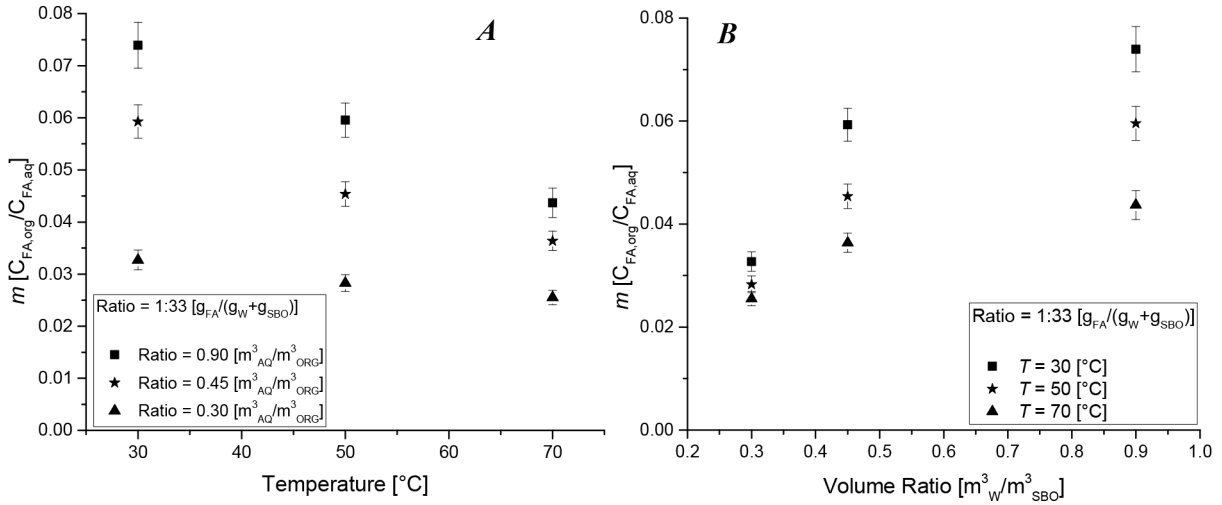

Figure 4. Experimental results obtained with a weight ratio of 0.03 $[g_{FA}/(g_{SBO} + g_W)]$. (A) Partition coefficient along temperature in parametric curves of volume ratio. (B) Partition coefficient along volume ratio in parametric curves of temperature.

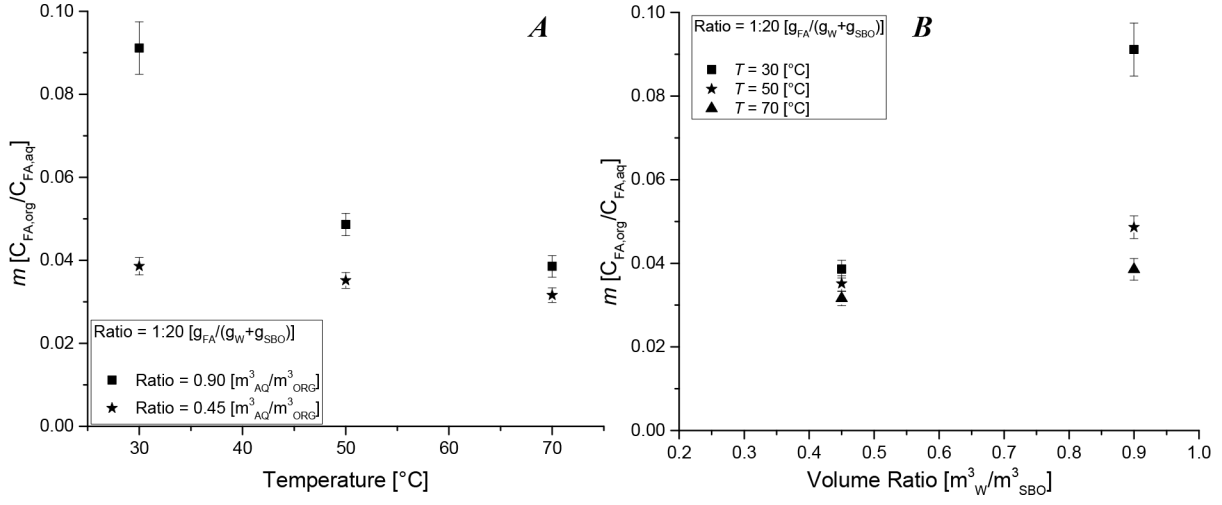

Figure 5. Experimental results obtained with a weight ratio 0.05 $[g_{FA}/(g_{SBO} + g_W)]$. (A) Partition coefficient along temperature in parametric curves of volume ratio. (B) Partition coefficient along volume ratio in parametric curves of temperature.

At first sight, revealed by Figures 2 and 3, it is possible to notice how the concentration of formic acid in the aqueous phase with time decreases from the initial concentration to a plateau. In the first stage of the experiment, in the decrement of the formic acid concentration, the mass transfer effect is the main player in the process. As the system was stirred at low rate (50 [rpm]), to guarantee homogeneity in each phase, the mass transfer coefficient obtained from these experiments can be considered to be the real coefficient for the water-soybean oil system at the operating conditions adopted in the present study. At the plateau, equilibrium conditions prevail in the system, and the difference of the formic acid concentration between the initial time and the plateau time is the amount which has left the aqueous phase and migrated to the organic one.

In order to reveal how the temperature and the water-to-oil weight ratio (indirectly volume ratio) influence the partition coefficient, the values of the experimental partition coefficients are displayed in parametric curves of the volume ratio and temperature (Figures 4 and 5). Starting from Figure 4, where the formic acid-to-soybean+water ratio is equal to 0.03 $[g_{FA}/(g_{SBO}+g_W)]$ (Table 1, entries 1−9), it is easy to recognize the linear decrement of the partition coefficient along the temperature as well as the increasing of its value with the increase of the volume ratio.

Figure 5 shows the results for the second set of experimental results where the weight amount of formic acid was equal to 0.05 $[g_{FA}/(g_{SBO} + g_W)]$ (Table 1, entries 10−15). It is possible to see that the trend in both cases remains.

The first interesting aspect to be observed from the experimental results is the absolute value of the partition coefficient (m) always being lower than 1, indicating the major tendency of formic acid to dissolve in water more eagerly than in soybean oil. The trend along the temperature decreases linearly independent of the volume ratio. This observation is quite unexpected compared to the empirical results obtained from SPARC,[31] as it implies that the amount of formic acid which migrates to the organic phase increases with temperature, despite that the solubility generally increases with temperature. Nevertheless, the observed behavior can be explained in terms of the relative solubility, and simply the relative solubility of formic acid in water increases more than the solubility of formic acid in soybean oil with temperature.

Rangarajan et al.[38] and Wu et al.[40] reported a decrement of the partition coefficient along with temperature measuring exper-

https://doi.org/10.1021/acs.iecr.3c01562
Ind. Eng. Chem. Res. 2023, 62, 13825−13836

imentally the acetic acid and formic acid partition coefficient in the water/soybean oil system, respectively. The volumetric ratio between the two phases seems to affect the partition coefficient more than the temperature. The related values increase by increasing the volume ratio of the two phases; similar behavior has been observed by other authors, too.[43,44] Furthermore, the order of magnitude obtained for the partition coefficient experimentally determined in the present work falls in the same range of the previous works dealing with a similar system, namely, soybean oil, water, and a carboxylic acid.[35,38,40] More specifically, by considering the work of Wu et al.,[40] where formic acid partition coefficient in a soybean oil/water system was experimentally determined, it is possible to notice the formic acid partition coefficient profiles along the temperature are the same, thus an equal temperature profile dependence Figure 6. Concerning the partition coefficient values, they present the same order of magnitude; the differences could be due to the differences in the adopted experimental conditions.

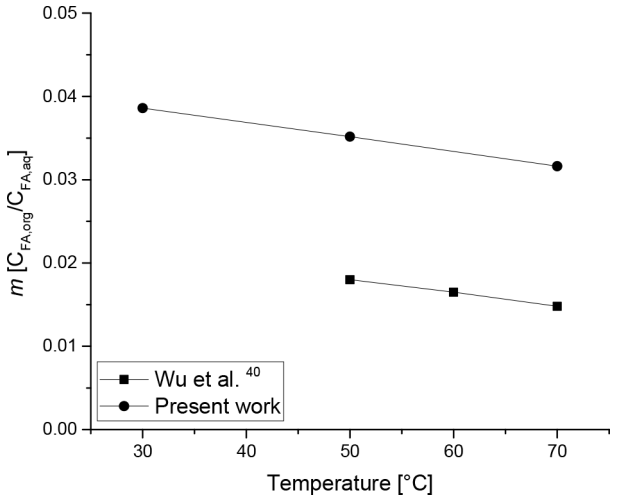

Figure 6. Experimental data sets comparison. (■) Wu et al.:[40] 0.06 $g_{FA}/(g_{SBO} + g_W)$ and 0.64 $[m^3_{AQ}/m^3_{SBO}]$. (●) Present work: 0.05 $g_{FA}/(g_{SBO} + g_W)$ and 0.45 $[m^3_{AQ}/m^3_{SBO}]$.

From the experimental data collected by us and displayed in the previous figures, it is possible to obtain an empirical expression for the partition coefficient in eq 10, where the dependence of the coefficient on the temperature is linearly decreasing and its dependence on the volumetric ratio of the phases is increasing. The agreement between the experimental and calculated data is depicted in Figures 2 & 3. Figure 2 shows how the mathematical model (continuous lines) describes the experimental data (discrete points) for the experiments at fixed formic acid-to-soybean+water weight ratio equal to 0.03 $[g_{FA}/(g_{SBO}+g_W)]$ at different water-to-oil volume ratio (or weight ratio, Table 1 entries 1−9). Figure 3 shows the very good agreement but at a formic acid-to-soybean+water weight ratio equal to 0.05 $[g_{FA}/(g_{SBO}+g_W)]$ (Table 1, entries 10−15). It is possible to see that the mathematical model fits the experimental data in a very accurate way considering both the temperature effect and the volume ratio dependency. The numerical values of the adjustable parameters obtained from the regression analysis are collected in Table 2, where both the 95 [%] confidence intervals and the correlation matrix are reported.

From the values of the confidence intervals, it is possible to see that the estimated parameters are associated with a very small error. The correlation matrix suggests that the correlation between the parameters is very minor. Finally, the overall agreement between the experimental data and the calculated value is shown in the parity plot displayed in Figure 7. The whole

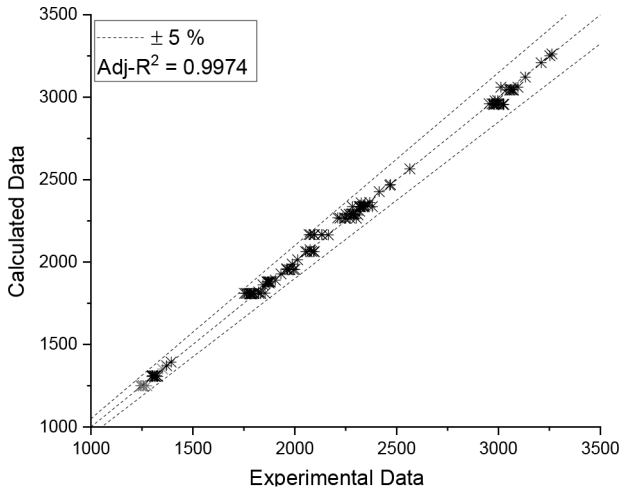

Figure 7. Parity plot for the empirical model results using both experimental and calculated concentrations.

set of data fall within the error boundary of 5%, and the adjusted coefficient of determination (R_{Adj}^2) exceeds 0.99. Thus, in support of the parity plot also the estimation statistics indicates a good agreement between the experimental and predicted data.

3.2. Elaboration of the Partition Coefficients. The partition coefficients of formic acid between water and soybean oil determined according to the procedure described in sections 2.4 and 2.6 are summarized in Table 3.

The agreement between them is illustrated in Figure 8 where the value of partition coefficient is compared with temperature and volume ratio when the formic acid-to-soybean+water weight ratio is fixed to 0.03 and 0.05 $[g_{FA}/(g_{SBO}+g_W)]$, respectively. The statistics is coupled also in this case, and a coefficient of determination (R^2) has been calculated and found equal to 0.80.

Table 3 also presents the results of the fits of the thermodynamic models UNIQUAC and NRTL to experimental

Table 2. Adjustable Parameters Are Estimated from Experimental Data

				Correlation matrix				
Parameter	Value	I.C. 95 [%]	Unit	a	b	c	d	k_{aq}
a	1.29	0.10	[-]	1.00				
b	0.19	0.03	[1/°C]	0.44	1.00			
c	5.80	0.50	[-]	−0.43	−0.81	1.00		
d	1.22	0.05	[-]	−0.63	−0.39	0.22	1.00	
k_m	0.08	0.02	[1/min]	−0.43	0.09	0.07	0.13	1.00

https://doi.org/10.1021/acs.iecr.3c01562
Ind. Eng. Chem. Res. 2023, 62, 13825−13836

Table 3. Comparison between the Experimental Numerical Values of the Partition Coefficient and Calculated Ones

Experiment	$H_{Exp} \pm$ I.C. 95%	${}^{A}H_{Calc}{}^{a}$	${}^{B}H_{Calc}{}^{a}$	${}^{C}H_{Calc}{}^{a}$
1	$(7.4 \pm 0.4) \times 10^{-2}$	7.4×10^{-2}	7.2×10^{-2}	7.4×10^{-2}
2	$(6.3 \pm 0.3) \times 10^{-2}$	4.5×10^{-2}	6.0×10^{-2}	6.4×10^{-2}
3	$(3.3 \pm 0.2) \times 10^{-2}$	3.2×10^{-2}	3.4×10^{-2}	3.3×10^{-2}
4	$(6.0 \pm 0.3) \times 10^{-2}$	5.7×10^{-2}	5.8×10^{-2}	5.8×10^{-2}
5	$(4.5 \pm 0.2) \times 10^{-2}$	3.8×10^{-2}	4.3×10^{-2}	4.6×10^{-2}
6	$(2.8 \pm 0.2) \times 10^{-2}$	2.8×10^{-2}	2.8×10^{-2}	2.9×10^{-2}
7	$(4.4 \pm 0.3) \times 10^{-2}$	4.7×10^{-2}	4.8×10^{-2}	4.2×10^{-2}
8	$(3.6 \pm 0.2) \times 10^{-2}$	3.3×10^{-2}	3.7×10^{-2}	3.6×10^{-2}
9	$(2.6 \pm 0.1) \times 10^{-2}$	2.5×10^{-2}	2.6×10^{-2}	2.6×10^{-2}
10	$(9.1 \pm 0.6) \times 10^{-2}$	7.3×10^{-2}	9.5×10^{-2}	9.3×10^{-2}
11	$(3.7 \pm 0.2) \times 10^{-2}$	4.5×10^{-2}	4.2×10^{-2}	3.8×10^{-2}
12	$(4.9 \pm 0.3) \times 10^{-2}$	5.8×10^{-2}	4.5×10^{-2}	4.9×10^{-2}
13	$(3.5 \pm 0.2) \times 10^{-2}$	3.9×10^{-2}	3.3×10^{-2}	3.4×10^{-2}
14	$(3.9 \pm 0.5) \times 10^{-2}$	4.7×10^{-2}	3.7×10^{-2}	3.9×10^{-2}
15	$(3.2 \pm 0.2) \times 10^{-2}$	3.3×10^{-2}	2.8×10^{-2}	3.0×10^{-2}

[a](A) MatLab; (B) UNIQUAC Thermodynamic model; (C) NRTL Thermodynamic model.

values of partition coefficients. The adjustable parameters of these models are summarized in Table 4, jointly with the coefficients of determination.

Table 4. Binary Adjustable Parameters Are Estimated from the Fit of Thermodynamic Models to Experimental Data

Parameter	Value	I.C. 95 [%]	Unit
UNIQUAC			
$\Delta u_{FA\text{-}W,aq}$	−2488	97	$[J \cdot mol^{-1}]$
$\Delta u_{W\text{-}FA,aq}$	10815	636	$[J \cdot mol^{-1}]$
$\Delta u_{FA\text{-}SBO,org}$	−3151	54	$[J \cdot mol^{-1}]$
$\Delta u_{SBO\text{-}FA,org}$	13949	74	$[J \cdot mol^{-1}]$
NRTL			
$\Delta g_{FA\text{-}W,aq}$	−3617	129	$[J \cdot mol^{-1}]$
$\Delta g_{W\text{-}FA,aq}$	14333	111	$[J \cdot mol^{-1}]$
$\Delta g_{FA\text{-}SBO,org}$	−3351	161	$[J \cdot mol^{-1}]$
$\Delta g_{SBO\text{-}FA,org}$	12613	213	$[J \cdot mol^{-1}]$

Figure 9 graphically expresses the results of the thermodynamic fits, with the partition coefficients also described as a function of the temperature and the volume ratio. Figure 10 presents a parity plot associated with the adjustment of the thermodynamic models.

The results from the fits of both thermodynamic models were quite similar and successful, with high values for the coefficients of determination: 0.99 (NRTL) and 0.97 (UNIQUAC). The visual tendency of the fits expressed in Figure 9 also corroborates the conclusion that both models fit very satisfactorily the data presented here, following the tendency of the experimental data.

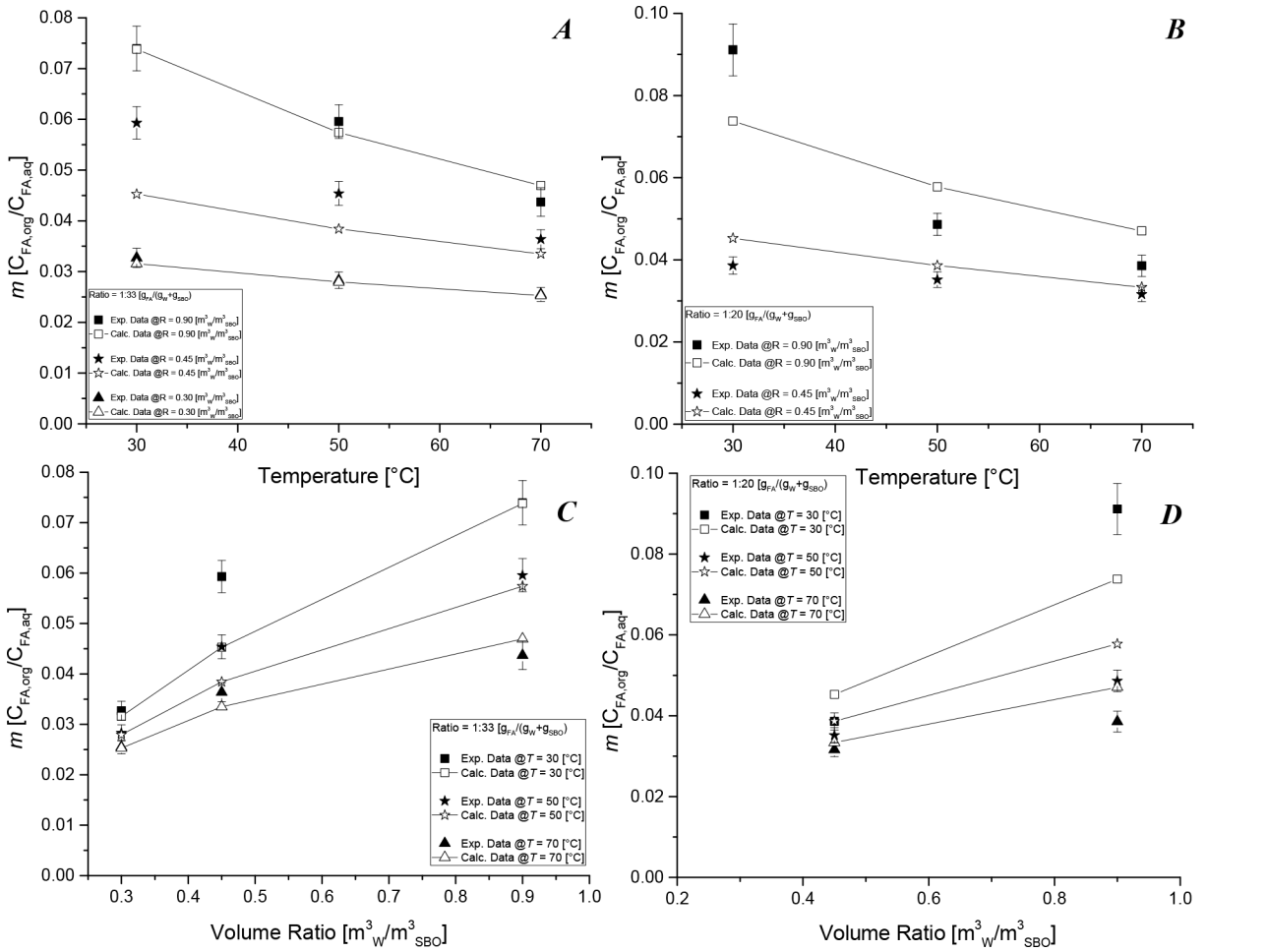

Figure 8. Experimental and predicted value of partition coefficient for a formic acid-to-soybean + water mixture with a weight ratio 0.03 (**A**, **C**) and 0.05 (**B**, **D**).

https://doi.org/10.1021/acs.iecr.3c01562
Ind. Eng. Chem. Res. 2023, 62, 13825−13836

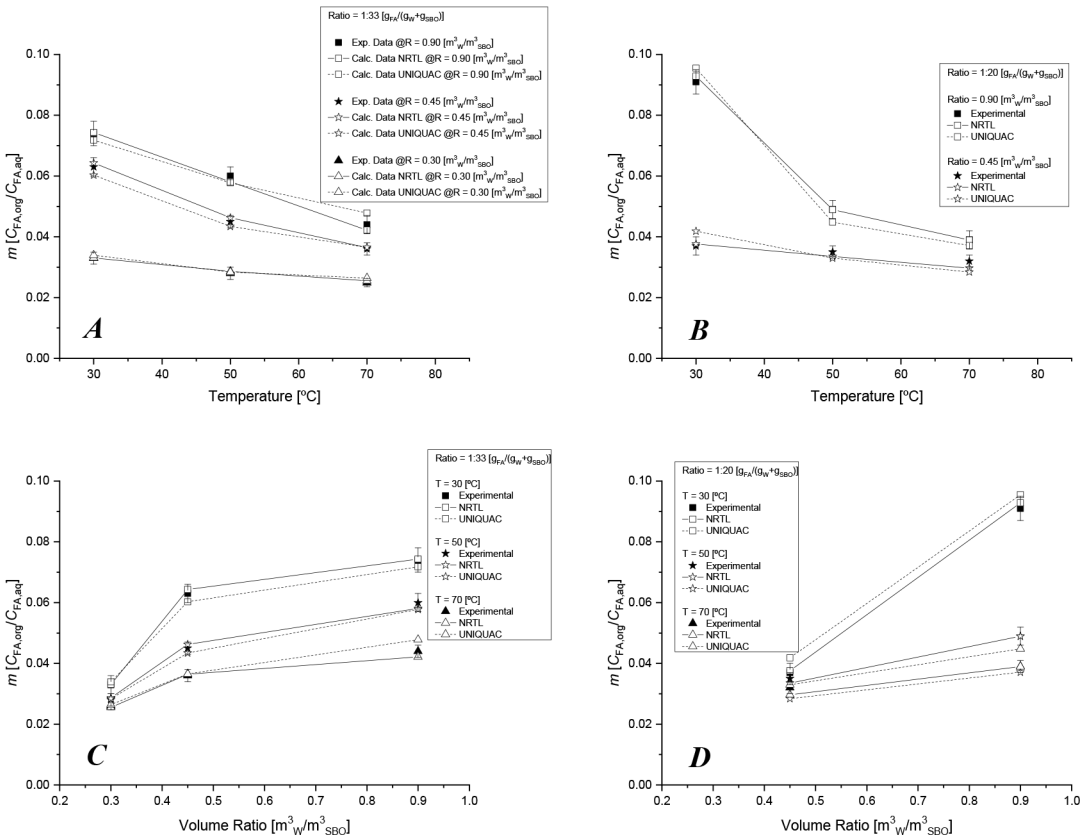

Figure 9. Experimental and predicted value (thermodynamic models) of partition coefficient for a formic acid-to-soybean+water mixture with a weight ratio 0.03 (**A**, **C**) and 0.05 (**B**, **D**).

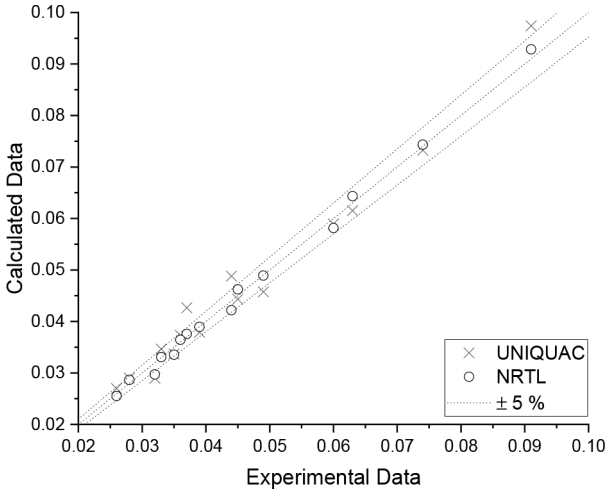

Figure 10. Parity plot for the thermodynamic model results using both experimental and calculated partition coefficients.

The literature showed that both NRTL and UNIQUAC models were able to correlate satisfactorily the partition coefficient values for acetic acid in systems containing soybean oil and water,[35] and olive oil, epoxidized olive oil, hydrogen peroxide, and water.[37] Particularly, the NRTL model tends to a good agreement with experimental data for systems that present partially miscible substances.

The two models resulted in both positive and negative values for the characteristic energies. It is notable that the characteristic energies agree in terms of signal and order of magnitude for both thermodynamic models tested, considering the same pair of substances. The results obtained here agree substantially with the UNIQUAC parameters from Janković et al.,[37] in which the characteristic energy between acetic acid and water, and between acetic acid and olive oil, are both negative (−4950 and −2399 J/mol, respectively), while the characteristic energy between water and acetic acid, and between olive oil and acetic acid, are both positive (15164 and 6073 J/mol, respectively). The present results also agree with the signals of the characteristic energies presented in the literature, only for the organic phase: Janković et al.[37] reported, for the NRTL model, −1796 J/mol for the characteristic energy between acetic acid and olive oil and 239 J/mol for the characteristic energy between olive oil and acetic acid; Sinadinović-Fišer and Janković[35] reported, for UNIQUAC, −5278 J/mol for the characteristic energy between acetic acid and soybean oil and 10669 J/mol between soybean oil and acetic acid.

Although the signals of the characteristic energies of the NRTL and UNIQUAC models could suggest the behavior of interactions between two different molecules compared with two molecules of the same substance, these values need to be interpreted carefully. For example, in the aqueous phase, there are several possible complexes derived from interactions through hydrogen bonds between formic acid and water molecules, and the interaction energy between them depends on the structure of the complex formed.[52]

However, the fit of the partition coefficients through models for activity coefficient shows great importance to enable the prediction of other thermodynamic properties related to the studied system, as well as the possibility to insert the binary parameters into process simulators typically used in the chemical industry.

https://doi.org/10.1021/acs.iecr.3c01562
Ind. Eng. Chem. Res. 2023, 62, 13825−13836

4. CONCLUSIONS

Experimental determination of the formic acid partition coefficient in the soybean oil/water system was carried out in the present work. The influence of the main parameters, the temperature, the water-to-soybean oil weight ratio, and the formic acid-to-soybean+water weight ratio on the partition coefficient was investigated. The experimental results revealed a higher solubility of formic acid in water compared to that of the soybean oil. This behavior is pronounced at higher temperatures where the absolute value of the partition coefficient decreased, showing an increase of a more profound solubility in water than in soybean oil. Conversely, by increasing the water-to-oil volume ratio (or weight ratio), the partition coefficient increased. This might be addressed with regard to the maximum solubility of formic acid in soybean oil. Finally, the proportion of formic acid-to-soybean oil+water appeared to have a minor effect. The experimental data collected during the different sets of experiments were successfully described by the mathematical model proposed, and an equation to predict the partition coefficient of the formic acid in the water/soybean oil system was proposed. The former equation takes the effect of the temperature and volume ratio into account. The results of both the empirical model and the partition coefficient equation are supported by estimation statistics. The thermodynamic models UNIQUAC and NRTL were also applied to fit the partition coefficient values, with estimation of binary parameters and satisfactory fits from both models.

■ ASSOCIATED CONTENT

Supporting Information

The Supporting Information is available free of charge at https://pubs.acs.org/doi/10.1021/acs.iecr.3c01562.

UNIQUAC and NRTL derivation (PDF)

■ AUTHOR INFORMATION

Corresponding Authors

Vincenzo Russo − *Department of Chemical Sciences, University of Naples Federico II, IT-80126 Napoli, Italy; Laboratory of Industrial Chemistry and Reaction Engineering (TKR), Åbo Akademi, FI-20500 Åbo/Turku, Finland;* orcid.org/0000-0002-1867-739X; Email: v.russo@unina.it

Martino Di Serio − *Department of Chemical Sciences, University of Naples Federico II, IT-80126 Napoli, Italy;* orcid.org/0000-0003-4489-7115; Email: diserio@unina.it

Authors

Gustavo V. Olivieri − *Department of Chemical Engineering, Escola Politécnica, Universidade de São Paulo, 05508-010 São Paulo, Brazil; Department of Chemical Engineering, Centro Universitário FEI, 09850-901 São Bernardo do Campo, Brazil;* orcid.org/0000-0001-6373-4181

Tommaso Cogliano − *Department of Chemical Sciences, University of Naples Federico II, IT-80126 Napoli, Italy; Laboratory of Industrial Chemistry and Reaction Engineering (TKR), Åbo Akademi, FI-20500 Åbo/Turku, Finland;* orcid.org/0000-0001-6225-6157

Ricardo Belchior Torres − *Department of Chemical Engineering, Centro Universitário FEI, 09850-901 São Bernardo do Campo, Brazil;* orcid.org/0000-0002-0791-4775

Rosa Turco − *Department of Chemical Sciences, University of Naples Federico II, IT-80126 Napoli, Italy;* orcid.org/0000-0002-2681-4286

Tapio Salmi − *Laboratory of Industrial Chemistry and Reaction Engineering (TKR), Åbo Akademi, FI-20500 Åbo/Turku, Finland;* orcid.org/0000-0002-9271-7425

Riccardo Tesser − *Department of Chemical Sciences, University of Naples Federico II, IT-80126 Napoli, Italy;* orcid.org/0000-0001-7002-7194

Reinaldo Giudici − *Department of Chemical Engineering, Escola Politécnica, Universidade de São Paulo, 05508-010 São Paulo, Brazil; Department of Chemical Engineering, Centro Universitário FEI, 09850-901 São Bernardo do Campo, Brazil;* orcid.org/0000-0001-6544-7098

Complete contact information is available at: https://pubs.acs.org/10.1021/acs.iecr.3c01562

Notes

The authors declare no competing financial interest.

■ ACKNOWLEDGMENTS

The authors acknowledge the grant PRIN: Progetti di Ricerca di Interesse Nazionale − Bando 2017 -prot. No. 2017KBTK93 "CARDoon valorisation by InteGrAted biorefiNery (CARDIGAN)" of Italian Ministero dell'Istruzione dell'Università e della Ricerca for the financial support. Financial support provided by Jenny and Antti Wihuri Foundation and Academy of Finland (Academy Professor grants 319002, 320115, and 34053) are gratefully acknowledged. This work was also supported by the São Paulo Research Foundation (FAPESP, grant Nos. 2019/00298-7 and 2022/01982-0).

■ NOTATION

A = Lewis cell cross-section area, [m^2]
a, b, c, d = Adjustable parameters
a_{sp} = Specific interfacial area [m^2/m^3]
$C^*_{i,j}$ = Concentration compound "i" at the interphase in the phase "j", [mol/m^3_j]
$C_{i,j}$ = Concentration compound "i" in the phase "j", [mol/m^3_j]
f_{NaOH} = Correction factor, [-]
$G_{i\text{-}k,j}$ = Binary parameter between the compounds "i" and "k" in the phase "j", [-]
m = Partition coefficient [-]
ID = Internal diameter of the Lewis cell, [m]
$J_{i,j}$ = Compound "i" molar flux in the phase "j", [$mol/(m^3_j \times min)$]
$k_{FA,i}$ = Formic acid mass transfer coefficient in the phase "i", [m/min]
l_i, q_i, q'_i, r_i = Parameters related to the size and surface area of the molecules of the compound "i", [-]
M_i = Molar mass of compound "i", [kg/mol]
w_i = Mass weigh of compound "i", [kg]
R = Universal constant for gases, [J/(mol × K)]
T_r = Reactor temperature, [°C or K]
V_i = Volume of phase "i", [m^3]
$x_{i,j}$ = Molar fraction of the compound "i" in the phase "j" [-]

■ GREEK LETTERS

$\alpha_{i\text{-}k,j}$ = Binary parameter associated with the nonrandomness between the compounds "i" and "k" in the phase "j", [-]
$\gamma_{i,j}$ = Activity coefficient of the compound "i" in the phase "j", [-]

$\Delta u_{i\text{-}k,j}$, $\Delta g_{i\text{-}k,j}$ = Characteristic energies between the compounds "i" and "k" in the phase "j", [J/mol]
$\theta_{i,j}$, $\theta'_{i,j}$ = Area fractions of the compound "i" in the phase "j", [-]
ρ_i = Phase "i" density, [kg/m^3]
$\rho_{m,i}$ = Phase "i" molar density, [mol/m^3]
$\tau_{i\text{-}k,j}$ = Binary parameter between the compounds "i" and "k" in the phase "j", [-]
$\Phi_{i,j}$ = Segment fraction of the compound "i" in the phase "j", [-]

STATISTICAL PARAMETERS

Cor_{ij} = Correlation matrix of the adjustable parameters "i" and "j"
J = Jacobian matrix
k = Number of adjustable parameters
n = Number of experimental observation
N = Number of experimental tests
OF = Objective function
R^2 = Coefficient of determination
R^2_{Adj} = Adjusted coefficient of determination
s = Standard deviation
V_{ij} = Covariance matrix of the adjustable parameters "i" and "j"
$\overline{y}$ = Average value of the experimental observation
$\hat{y}_i$ = Value of the calculated observation during the experiment "i"
y_i = Value of the experimental observation during the experiment "i"

REFERENCES

(1) Datta, J.; Włoch, M. Selected Biotrends in Development of Epoxy Resins and Their Composites. *Polym. Bull.* **2014**, *71* (11), 3035−3049.
(2) Desroches, M.; Escouvois, M.; Auvergne, R.; Caillol, S.; Boutevin, B. From Vegetable Oils to Polyurethanes: Synthetic Routes to Polyols and Main Industrial Products. *Polym. Rev.* **2012**, *52* (1), 38−79.
(3) Wang, X. L.; Chen, L.; Wu, J. N.; Fu, T.; Wang, Y. Z. Flame-Retardant Pressure-Sensitive Adhesives Derived from Epoxidized Soybean Oil and Phosphorus-Containing Dicarboxylic Acids. *ACS Sustain. Chem. Eng.* **2017**, *5* (4), 3353−3361.
(4) Li, A.; Li, K. Pressure-Sensitive Adhesives Based on Epoxidized Soybean Oil and Dicarboxylic Acids. *ACS Sustain. Chem. Eng.* **2014**, *2* (8), 2090−2096.
(5) Hosney, H.; Nadiem, B.; Ashour, I.; Mustafa, I.; El-Shibiny, A. Epoxidized Vegetable Oil and Bio-Based Materials as PVC Plasticizer. *J. Appl. Polym. Sci.* **2018**, *135* (20), 46270.
(6) Zhang, C.; Garrison, T. F.; Madbouly, S. A.; Kessler, M. R. Recent Advances in Vegetable Oil-Based Polymers and Their Composites. *Prog. Polym. Sci.* **2017**, *71*, 91−143.
(7) Paraskar, P. M.; Prabhudesai, M. S.; Hatkar, V. M.; Kulkarni, R. D. Vegetable Oil Based Polyurethane Coatings − A Sustainable Approach: A Review. *Prog. Org. Coatings* **2021**, *156* (April), No. 106267.
(8) Kumar, S. Recent Developments of Biobased Plasticizers and Their Effect on Mechanical and Thermal Properties of Poly(Vinyl Chloride): A Review. *Ind. Eng. Chem. Res.* **2019**, *58* (27), 11659−11672.
(9) Tan, S. G.; Chow, W. S. Biobased Epoxidized Vegetable Oils and Its Greener Epoxy Blends: A Review Biobased Epoxidized Vegetable Oils and Its Greener Epoxy Blends: A Review. *Polymer-Plastics Technology and Engineering* **2010**, *49* (15), 1581−1590, DOI: 10.1080/03602559.2010.512338.
(10) Turco, R.; Vitiello, R.; Tesser, R.; Vergara, A.; Andini, S.; Di Serio, M. Niobium Based Catalysts for Methyl Oleate Epoxidation Reaction. *Top. Catal.* **2017**, *60* (15−16), 1054−1061.
(11) Wei, X.; Cheng, Q.; Sun, T.; Tong, S.; Meng, L. Enhanced Epoxidation of Soybean Oil by Novel Al_2O_3−ZrO_2−TiO_2 Solid Acid Catalyst. *Appl. Organomet. Chem.* **2021**, *35* (1), No. e6063, DOI: 10.1002/aoc.6063.
(12) Chen, C.; Cai, L.; Li, L.; Bao, L.; Lin, Z.; Wu, G. Heterogeneous and Non-Acid Process for Production of Epoxidized Soybean Oil from Soybean Oil Using Hydrogen Peroxide as Clean Oxidant over TS-1 Catalysts. *Microporous Mesoporous Mater.* **2019**, *276* (Sept), 89−97.
(13) Turco, R.; Bonelli, B.; Armandi, M.; Spiridigliozzi, L.; Dell'Agli, G.; Deorsola, F. A.; Esposito, S.; Di Serio, M. Active and Stable Ceria-Zirconia Supported Molybdenum Oxide Catalysts for Cyclooctene Epoxidation: Effect of the Preparation Procedure. *Catal. Today* **2020**, *345* (Oct), 201−212.
(14) Farias, M.; Martinelli, M.; Bottega, D. P. Epoxidation of Soybean Oil Using a Homogeneous Catalytic System Based on a Molybdenum (VI) Complex. *Appl. Catal. A Gen.* **2010**, *384* (1−2), 213−219.
(15) Tiozzo, C.; Bisio, C.; Carniato, F.; Marchese, L.; Gallo, A.; Ravasio, N.; Psaro, R.; Guidotti, M. Epoxidation with Hydrogen Peroxide of Unsaturated Fatty Acid Methyl Esters over Nb(V)-Silica Catalysts. *Eur. J. Lipid Sci. Technol.* **2013**, *115* (1), 86−93.
(16) Sepulveda, J.; Teixeira, S.; Schuchardt, U. Alumina-Catalyzed Epoxidation of Unsaturated Fatty Esters with Hydrogen Peroxide. *Appl. Catal. A Gen.* **2007**, *318*, 213−217.
(17) Campanella, A.; Baltanás, M. A.; Capel-Sánchez, M. C.; Campos-Martín, J. M.; Fierro, J. L. G. Soybean Oil Epoxidation with Hydrogen Peroxide Using an Amorphous Ti/SiO2 Catalyst. *Green Chem.* **2004**, *6* (7), 330−334.
(18) Perez-Sena, W. Y.; Wärnå, J.; Eränen, K.; Tolvanen, P.; Estel, L.; Leveneur, S.; Salmi, T. Use of Semibatch Reactor Technology for the Investigation of Reaction Mechanism and Kinetics: Heterogeneously Catalyzed Epoxidation of Fatty Acid Esters. *Chem. Eng. Sci.* **2021**, *230* (xxxx), No. 116206.
(19) Turco, R.; Pischetola, C.; Tesser, R.; Andini, S.; Di Serio, M. New Findings on Soybean and Methylester Epoxidation with Alumina as the Catalyst. *RSC Adv.* **2016**, *6* (38), 31647−31652.
(20) Santacesaria, E.; Turco, R.; Russo, V.; Tesser, R.; Di Serio, M. Soybean Oil Epoxidation: Kinetics of the Epoxide Ring Opening Reactions. *Processes* **2020**, *8* (9), 1134.
(21) Cai, X.; Zheng, J. L.; Aguilera, A. F.; Vernières-Hassimi, L.; Tolvanen, P.; Salmi, T.; Leveneur, S. Influence of Ring-Opening Reactions on the Kinetics of Cottonseed Oil Epoxidation. *Int. J. Chem. Kinet.* **2018**, *50* (10), 726−741.
(22) Campanella, A.; Baltanás, M. A. Degradation of the Oxirane Ring of Epoxidized Vegetable Oils in Liquid-Liquid Heterogeneous Reaction Systems. *Chem. Eng. J.* **2006**, *118* (3), 141−152.
(23) Campanella, A.; Baltanás, M. A. Degradation of the Oxirane Ring of Epoxidized Vegetable Oils in Liquid-Liquid Systems: I. Hydrolysis and Attack by H2O2. *Lat. Am. Appl. Res.* **2005**, *35* (3), 205−210.
(24) Campanella, A.; Baltanás, M. A. Degradation of the Oxirane Ring of Epoxidized Vegetable Oils with Solvated Acetic Acid Using Cation-Exchange Resins. *Eur. J. Lipid Sci. Technol.* **2004**, *106* (8), 524−530.
(25) Cai, X.; Zheng, J. L.; Aguilera, A. F.; Vernières-Hassimi, L.; Tolvanen, P.; Salmi, T.; Leveneur, S. Influence of Ring-Opening Reactions on the Kinetics of Cottonseed Oil Epoxidation. *Int. J. Chem. Kinet.* **2018**, *50* (10), 726−741.
(26) Bakhtiar, C.; Hardy, D. T. Epoxides. *Lect. Org. Chem.* **1997**, 137−140.
(27) Cogliano, T.; Russo, V.; Turco, R.; Santacesaria, E.; Di Serio, M.; Salmi, T.; Tesser, R. Revealing the Role of Stabilizers in H2O2 for the Peroxyformic Acid Synthesis and Decomposition Kinetics. *Chem. Eng. Sci.* **2022**, *251*, No. 117488.
(28) Aguilera, A. F.; Tolvanen, P.; Wärnå, J.; Leveneur, S.; Salmi, T. Kinetics and Reactor Modelling of Fatty Acid Epoxidation in the Presence of Heterogeneous Catalyst. *Chem. Eng. J.* **2019**, *375* (May), No. 121936.
(29) Ramírez, L. M.; Cadavid, J. G.; Orjuela, A.; Gutiérrez, M. F.; Bohórquez, W. F. Epoxidation of Used Cooking Oils: Kinetic Modeling and Reaction Optimization. *Chem. Eng. Process. - Process Intensif.* **2022**, *176* (Feb), No. 108963.

https://doi.org/10.1021/acs.iecr.3c01562
Ind. Eng. Chem. Res. 2023, 62, 13825−13836

(30) Santacesaria, E.; Turco, R.; Russo, V.; Di Serio, M.; Tesser, R. Kinetics of Soybean Oil Epoxidation in a Semibatch Reactor. *Ind. Eng. Chem. Res.* **2020**, *59* (50), 21700−21711.
(31) Santacesaria, E.; Tesser, R.; Di Serio, M.; Turco, R.; Russo, V.; Verde, D. A Biphasic Model Describing Soybean Oil Epoxidation with H2O2 in a Fed-Batch Reactor. *Chem. Eng. J.* **2011**, *173* (1), 198−209.
(32) Olivieri, G. V.; De Quadros, J. V.; Giudici, R. Epoxidation Reaction of Soybean Oil: Experimental Study and Comprehensive Kinetic Modeling. *Cite This Ind. Eng. Chem. Res.* **2020**, *59*, 18808−18823.
(33) Zheng, J. L.; Wärnå, J.; Salmi, T.; Burel, F.; Taouk, B.; Leveneur, S. Kinetic Modeling Strategy for an Exothermic Multiphase Reactor System: Application to Vegetable Oils Epoxidation Using Prileschajew Method. *AIChE J.* **2016**, *62* (3), 726−741.
(34) Turco, R.; Tesser, R.; Russo, V.; Cogliano, T.; Di Serio, M.; Santacesaria, E. Epoxidation of Linseed Oil by Performic Acid Produced In Situ. *Ind. Eng. Chem. Res.* **2021**, *60* (46), 16607−16618.
(35) Sinadinović-Fišer, S.; Janković, M. Prediction of the Partition Coefficient for Acetic Acid in a Two-Phase System Soybean Oil-Water. *JAOCS, J. Am. Oil Chem. Soc.* **2007**, *84* (7), 669−674.
(36) Janković, M.; Sinadinović-Fišer, S. Prediction of the Chemical Equilibrium Constant for Peracetic Acid Formation by Hydrogen Peroxide. *JAOCS, J. Am. Oil Chem. Soc.* **2005**, *82* (4), 301−303.
(37) Janković, M. R.; Govedarica, O. M.; Sinadinović-Fišer, S. V.; Pavličević, J. M.; Teofilović, V. B.; Vukić, N. R. Liquid−Liquid Equilibrium Constant for Acetic Acid in an Olive Oil−Epoxidized Olive Oil−Acetic Acid−Hydrogen Peroxide−Water System. *Hem. Ind.* **2016**, *70* (2), 165−175.
(38) Rangarajan, B.; Havey, A.; Grulke, E. A.; Culnan, P. D. Kinetic Parameters of a Two-Phase Model for in Situ Epoxidation of Soybean Oil. *J. Am. Oil Chem. Soc.* **1995**, *72* (10), 1161−1169.
(39) Janković, M.; Sinadinović-Fišer, S.; Lamshoeft, M. Liquid-Liquid Equilibrium Constant for Acetic Acid in an Epoxidized Soybean Oil-Acetic Acid-Water System. *JAOCS, J. Am. Oil Chem. Soc.* **2010**, *87* (5), 591−600.
(40) Wu, Z.; Nie, Y.; Chen, W.; Wu, L.; Chen, P.; Lu, M.; Yu, F.; Ji, J. Mass Transfer and Reaction Kinetics of Soybean Oil Epoxidation in a Formic Acid-Autocatalyzed Reaction System. *Can. J. Chem. Eng.* **2016**, *94* (8), 1576−1582.
(41) Janković, M. R.; Govedarica, O. M.; Sinadinović-Fišer, S. V. The Epoxidation of Linseed Oil with in Situ Formed Peracetic Acid: A Model with Included Influence of the Oil Fatty Acid Composition. *Ind. Crops Prod.* **2020**, *143* (Nov), No. 111881.
(42) Fogler, H. S. *Elements of Chemical Reaction Engineering,* 3rd ed.; Prentice-Hall of India, 2004.
(43) Marcos, J. C.; Fonseca, L. P.; Ramalho, M. T.; Cabral, J. M. S. Variation of Penicillin Acylase Partition Coefficient with Phase Volume Ratio in Poly(Ethylene Glycol)-Sodium Citrate Aqueous Two-Phase Systems. *J. Chromatogr. B Biomed. Appl.* **1998**, *711* (1−2), 295−299.
(44) Spelzini, D.; Picó, G.; Farruggia, B. Dependence of Chymosin and Pepsin Partition Coefficient with Phase Volume and Polymer Pausidispersity in Polyethyleneglycol-Phosphate Aqueous Two-Phase System. *Colloids Surfaces B Biointerfaces* **2006**, *51* (1), 80−85.
(45) Cratin, P. D. Partitioning at the Liquid-Liquid Interface. *Ind. Eng. Chem.* **1968**, *60* (9), 14−19.
(46) Prausnitz, J. M.; Lichtenthaler, R. N.; de Azevedo, E. G. *Molecular Thermodynamics of Fluid-Phase Equilibria,* 3rd ed.; Prentice Hall PTR: NJ, 1999.
(47) Easton, M. M. F.; Mitchell, A. G.; Wynne-Jones, W. F. K. The Behaviour of Mixtures of Hydrogen Peroxide and Water Part 1.-Determination of the Densities of Mixtures of Hydrogene Peroxide and Water. *Trans. Faraday Soc.* **1952**, *48*, 796−801.
(48) Thomaz, A. Fats and Fatty Oils. In *Ullmann's Encyclopedia of Industrial Chemistry;* Wiley-VCH: Weinheim, Germany, 2011; pp 1−73.
(49) Sommer, T.; Trejbal, J.; Kopecký, D. Isobaric and Isothermal Vapor-Liquid Equilibria for the Binary System of Water + Formic Acid at 99.41 KPa, 388.15 K, and 398.15 K. *J. Chem. Eng. Data* **2016**, *61* (10), 3398−3405.
(50) Trofimova, M.; Sadaev, A.; Samarov, A.; Toikka, M.; Toikka, A. Solubility, Liquid-Liquid Equilibrium and Critical States for the Quaternary System Formic Acid − Ethanol − Ethyl Formate − Water at 298.15 K and 308.15 K. *Fluid Phase Equilib.* **2019**, *485*, 111−119.
(51) Fang, J.; Zheng, T.; Wu, Z.; Wu, L.; Xie, Q.; Xia, F.; Lu, M.; Nie, Y.; Ji, J. Liquid−Liquid Equilibrium for Systems Containing Epoxidized Oils, Formic Acid, and Water: Experimental and Modeling. *JAOCS, J. Am. Oil Chem. Soc.* **2019**, *96* (8), 955−965.
(52) Zhou, Z.; Shi, Y.; Zhou, X. Theoretical Studies on the Hydrogen Bonding Interaction of Complexes of Formic Acid with Water. *J. Phys. Chem. A* **2004**, *108* (5), 813−822.

https://doi.org/10.1021/acs.iecr.3c01562
Ind. Eng. Chem. Res. 2023, 62, 13825−13836